Environ Monit Assess (2021) 193: 203
https://doi.org/10.1007/s10661-021-08982-7

Assessment of iron-rich tailings via portable X-ray fluorescence spectrometry: the Mariana dam disaster, southeast Brazil

Gabriel W. D. Ferreira · Bruno T. Ribeiro · David C. Weindorf · Barbara I. Teixeira · Somsubhra Chakraborty · Bin Li · Luiz Roberto G. Guilherme · José Roberto S. Scolforo

Received: 11 June 2020 / Accepted: 25 February 2021 / Published online: 22 March 2021

Abstract On November 5, 2015, the *Fundão* dam collapsed and released >60 million m^3 of iron-rich mining sediments into the *Doce* river basin, covering >1000 ha of floodplain soils across ~80 km from the rupture. The characterization of alluvial mud covering and/or mixed with native soil is a priority for successful environmental rehabilitation. Portable X-ray fluorescence (pXRF) spectrometry was used to (1) assess the elemental composition of native soils and alluvial mud across impacted riparian areas; and 2) predict fertility properties of the mud and soils that are crucial for environmental rehabilitation and vegetation establishment (e.g., pH, available macro and micronutrients, cation exchange capacity, organic matter). Native soils and alluvial mud were sampled across impacted areas and analyzed via pXRF and conventional laboratory methods. Random forest (RF) regression was used to predict fertility properties using pXRF data for pooled soil and alluvial mud samples. Mud and native surrounding soils were clearly differentiated based on chemical properties determined via pXRF (mainly SiO_2, Al_2O_3, Fe_2O_3, TiO_2, and MnO). The pXRF data and RF models successfully predicted pH for pooled samples ($R^2 = 0.80$). Moderate predictions were

G. W. D. Ferreira (✉) · B. I. Teixeira · J. R. S. Scolforo
Department of Forest Sciences, Federal University of Lavras, Minas Gerais State, Doutor Sylvio Menicucci Avenue, Lavras 37200-900, Brazil
e-mail: gferreira@uga.edu

G. W. D. Ferreira
Savannah River Ecology, University of Georgia, P O Drawer E, SC, Aiken 29802, USA

B. T. Ribeiro · L. R. G. Guilherme
Department of Soil Science, Federal University of Lavras, Minas Gerais State, Doutor Sylvio Menicucci Avenue, Lavras 37200-900, Brazil

B. T. Ribeiro · D. C. Weindorf
Department of Plant and Soil Science, Texas Tech University, Bayer Plant Science Building, Room 211A, 2911 15th Street, Lubbock, TX 79409, USA

D. C. Weindorf
Department of Earth and Atmospheric Sciences, Central Michigan University, Mount Pleasant, MI 48859, USA

S. Chakraborty
Agricultural and Food Engineering Department, Indian Institute of Technology , Kharagpur, West Bengal 721302, India

B. Li
Department of Experimental Statistics, Louisiana State University, Baton Rouge, LA 70802, USA

obtained for soil organic matter ($R^2 = 0.53$) and cation exchange capacity ($R^2 = 0.54$). Considering the extent of impacted area and efforts required for successful environmental rehabilitation, the pXRF spectrometer showed great potential for screening impacted areas. It can assess total elemental composition, differentiate alluvial mud from native soils, and reasonably predict related fertility properties in pooled heterogeneous substrates (native soil + mud + river sediments).

Keywords Proximal sensors · PXRF · Mining activities · Samarco dam collapse · Random forest · Environmental monitoring

Introduction

On November 5, 2015, the *Fundão* dam located in Mariana, Minas Gerais, Brazil, collapsed and released >60 million m^3 of iron-rich mining sediments into the *Doce* river basin (Aires et al., 2018; Fernandes et al., 2016). The failure resulted in the destruction of two villages, 18 people dead, and >600 km of downstream effects which caused extensive ecological and social damage (Fernandes et al., 2016). This tragedy is considered the world's largest environmental calamity in terms of volume and magnitude from mining activities to date (Aires et al., 2018; Carmo et al., 2017; Fernandes et al., 2016). Most coarse materials were retained throughout the first 80 km downstream to the *Candonga* dam (Carmo et al., 2017). The river floodplains and margins were covered by iron ore tailings which changed soil chemical and physical properties and destroyed riparian vegetation (Silva Junior et al., 2018; Guerra et al., 2017; Omachi et al., 2018). The characterization of alluvial mud covering and/or mixed with native soil in riparian zones is a priority for successful environmental rehabilitation (Zago et al., 2019).

Several studies have investigated the magnitude of ecological impacts by mud deposition on water quality (Segura et al., 2016), fish and algae communities (Miranda & Marques, 2016), estuarine conditions (Gomes et al., 2017; Queiroz et al., 2018), riparian soils (Almeida et al., 2018; Davila et al., 2020; Guerra et al., 2017), and vegetation (Omachi et al., 2018). Previous studies performed on riparian soils identified low contamination potential (generally lower than environmental legislation thresholds in Brazil), although trace metal enrichment could be found in specific locations (Davila et al., 2020; Duarte et al., 2021; Guerra et al., 2017). However, the alluvial mud has different chemical properties than native soils of the area. Once mixed with soil, it can result in a material with unknown elemental composition and sorption/desorption dynamics that could affect both nutrient availability and heavy metal mobility (Almeida et al., 2018; Queiroz et al., 2018). Remarkably, a substantial amount of material is deposited on river floodplain margins, which increases the risk of redox oscillations due to water level fluctuations throughout the year and potentially uncertain elemental dynamics (Queiroz et al., 2018).

In addition to soil contamination assessment, another great challenge is the characterization of fertility properties to support successful revegetation and environmental rehabilitation. Considering the large floodplain impacted area (>1000 ha; Aires et al., 2018; Omachi et al., 2018), soil/mud characterization via standard laboratory methods can be costly and generate considerable toxic waste. Therefore, an accurate, low-cost, rapid, and environment-friendly characterization method is preferable and would warrant the establishment of detailed and adaptive field sampling schemes. Lately, portable X-ray fluorescence (pXRF) spectrometry has gained attention as a powerful tool for rapid soil elemental composition assessment and its ability to accurately predict ancillary soil properties such as pH, available nutrients, cation exchange capacity, and texture (Andrade et al., 2020; Lima et al., 2019; Sharma et al., 2014, 2015; Silva et al., 2020; Teixeira et al., 2020). Therefore, while pXRF can be useful for monitoring and rehabilitation efforts by combining elemental determination and fertility assessment, its applicability still requires empirical testing.

pXRF technology has been adopted worldwide for metals assessment in mining areas (Jang, 2010; Peinado et al., 2010). Results have been well correlated to conventional soil analysis like wet digestion (e.g., USEPA 3051a or USEPA 3052 methods) followed by atomic absorption spectrometry (AAS) or inductively coupled plasma optical emission spectroscopy (ICP-OES) quantification (Kilbride et al., 2006; Rouillon & Taylor, 2016). Effectively, by applying pXRF, the number of samples analyzed through conventional laboratory techniques could be reduced while producing accurate data for spatial interpolation (Horta et al., 2021). Besides

providing time, economic, and environmental benefits, pXRF can be used in both in situ or ex situ (Weindorf et al., 2014). Interest in tropical soil pXRF application is rapidly growing with a new compendium of tropical soil methods and applications just released (Silva et al., 2021). However, pXRF application, testing, and development in mining contaminated sites remain relatively scarce (Ribeiro et al., 2017; Silva et al., 2021).

The main objectives of this study were to (1) determine the total elemental composition of native soils and alluvial mud via pXRF across impacted riparian areas between the *Fundão* and *Candonga* dams, and (2) predict mud and soil fertility properties crucial for environmental rehabilitation and vegetation establishment such as pH, available macro and micronutrients, cation exchange capacity, and organic matter. We hypothesized that (1) pXRF can be used to successfully differentiate impacted from non-impacted areas based on geochemical signatures, and (2) pXRF data can be used to predict soil fertility properties such as pH, cation exchange capacity, and organic matter, in both native soil and alluvial mud, which have direct implications for remediation efforts on impacted areas.

Material and methods

Description of the study area

After the dam rupture on November 5, 2015, the iron-rich tailings traveled >600 km from the *Fundão* dam to the Atlantic Ocean in Linhares, Espírito Santo, Brazil (Fig. 1). The most impacted area comprised 15 km^2 of covered soil in the river margins and was concentrated along the first ~80 km downstream from the *Fundão* dam: (i) ~50 km down the *Gualaxo* river margins, (ii) 22 km in the *Carmo* river, (iii) and 2 km of the *Doce* river. The *Doce* river is dammed at its initial extension, creating the *Candonga* reservoir, where most coarse materials were deposited (Carmo et al., 2017). These areas are located in three municipalities within Minas Gerais: Mariana, Barra Longa, and Rio Doce. The *Fundão* dam is located in Mariana (20° 12′ S, 43° 27′ W; mean elevation 825 m asl). The *Candonga* reservoir is located in Rio Doce (20° 12′ S; 42° 51′ W; mean elevation 298 m asl). The climate of the impacted area is classified as Cwa per the Köppen classification (Alvares et al., 2013), with a mean annual temperature of 21.5° C and annual rainfall averaging 1200 mm. It is located in the *Quadrilátero Ferrífero* region, which is characterized by prevalence of itabirite and hematite (Selmi et al., 2009). Multiple soil classes occur in the *Doce* river basin (Guevara et al., 2018). Affected soils were mostly Cambisols and Fluvisols (IUSS Working Group WRB, 2015; Schaefer et al., 2016). However, due to the amount of tailings that covered native soils imparting significant chemical and physical changes therein, the soils covered by alluvial mud are being classified as Technosols (IUSS Working Group WRB, 2015; Schaefer et al., 2015, 2016).

Immediately after the dam rupture, emergency actions were employed to stabilize riverbanks and promote revegetation. Most riparian areas were amended with manure, fertilizer (NPK and single phosphate), and a seed mix (leguminous and gramineous). A detailed description of the emergency activities is given by Renova (2018).

Mud and soil sampling

The soil and/or mud samples were collected 2 years after the dam collapse (September–November of 2017) at 35 locations (~2 km apart from each other) across three different river sections (*Gualaxo*, *Carmo*, and *Doce*) from the *Fundão* dam to the *Candonga* reservoir (Fig. 1). At each sampling point, samples (0–20 cm layer; Abrahão & Marques, 2013) were collected in three different *sites* aligned perpendicular to the drainage line. *Site 1* was in river margin areas affected by alluvial mud deposition where emergency actions were employed. *Site 2* was in river margin impacted areas but where no emergency actions were undertaken. Most of these areas were still covered by native vegetation. *Site 3* was in adjacent soil at a higher slope position where the alluvial mud did not reach. These three *sites* are represented in Fig. 1. Geolocation of all collected samples was accomplished using a handheld global positioning system receiver with a horizontal accuracy of ~15 m.

Conventional soil fertility analyses

Samples were oven-dried at 60°C and passed through a 2-mm sieve for further analyses. The following analyses were performed according to the Brazilian Methods of Soil Analysis (Embrapa, 2011): soil reaction (pH), cation exchange capacity (CEC),

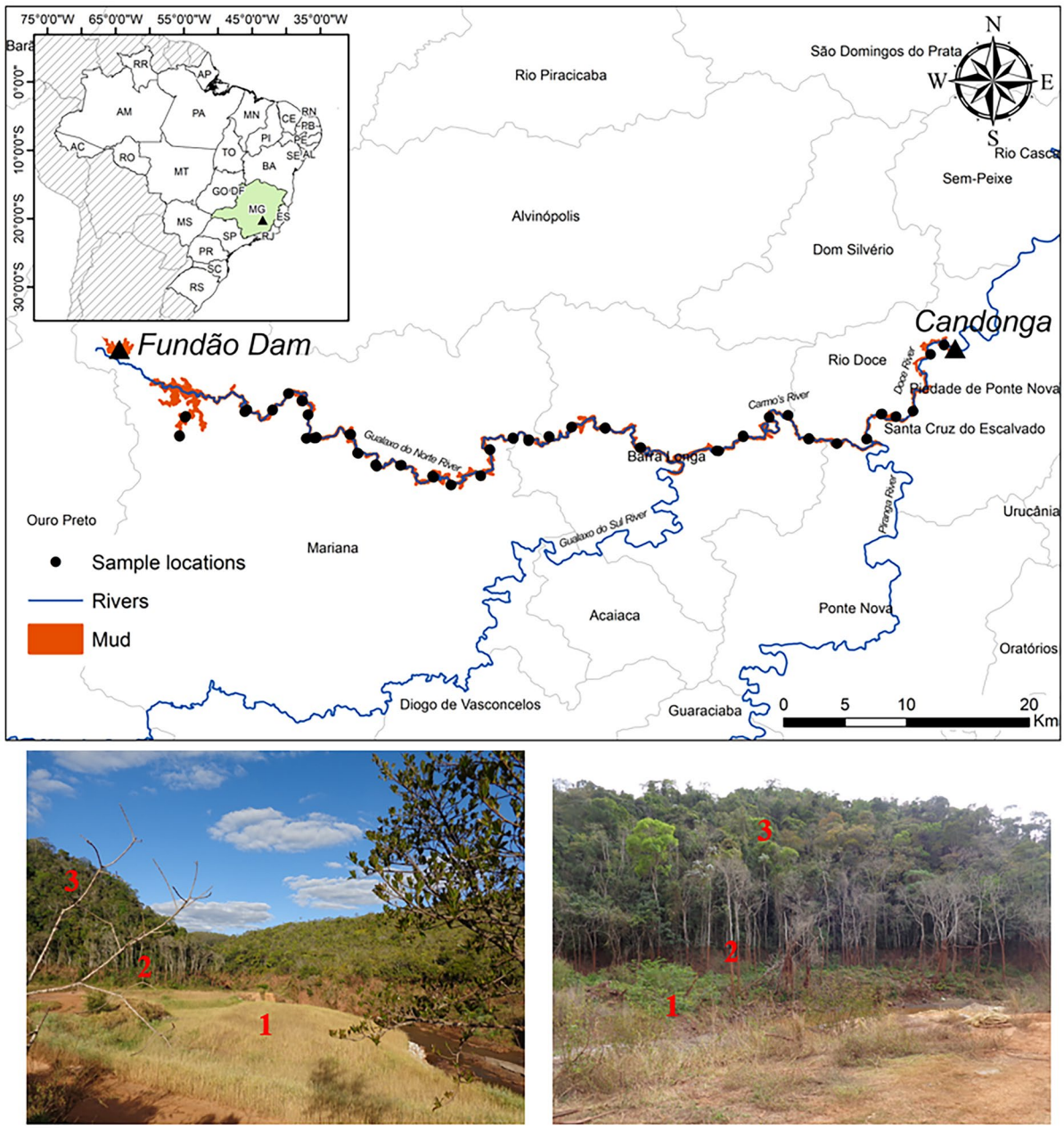

Fig. 1 Study area and sampling locations ($n = 35$) from the *Fundão* dam to the *Candonga* reservoir, with illustrations of the different sampling points (*sites*: 1, 2, and 3). *Site* 1—mud deposition with emergency actions; *Site* 2—mud deposition with no emergency actions; and *Site* 3—native surrounding soils

macro- and micronutrients, S-SO_4^{2-}, soil organic matter (SOM), and P-remaining (P-rem). Briefly, the soil pH was measured in a 1:2.5 (*v*/*v*) soil:water slurry after 15-min shaking and 1-h equilibration prior to reading with a benchtop pH meter (SevenEasy pH meter S20-K, Mettler Toledo, Barueri, SP, Brazil). Exchangeable cations (Ca^{2+}, Mg^{2+}, Al^{3+}, and Na^{+}) were extracted using 1.0 mol L^{-1} KCl at a 1:10 (*v*/*v*) soil/solution ratio. After shaking overnight (16 h), the samples were left to equilibrate for 1 h. Ca^{2+} and Mg^{2+}

were quantified in the supernatant via atomic absorption spectrometry using an AA Analyst 400 (Perkin Elmer, Waltham, MA, USA); Na^+ was quantified using a Digimed DM-62 flame photometer (Digimed, São Paulo, SP, Brazil); Al^{3+} was quantified by titration with 0.025 mol L^{-1} NaOH solution (Wright & Stuczynski, 1996). Mehlich-1 solution was used to extract exchangeable K, P, and plant-available micronutrients (Fe, Mn, Zn, and Cu). K was quantified via flame photometer, P by molybdenum blue colorimetry, and the micronutrients via atomic absorption spectrometry (Wright & Stuczynski, 1996). Soil organic matter was determined colorimetrically after digestion with potassium dichromate solution (Yeomans & Bremner, 1988). We calculated the effective cation exchange capacity (CEC1) as a sum of $Ca^{2+}+Mg^{2+}+K^{+}+Al^{3+}$; the potential cation exchange capacity (CEC2) as a sum of $Ca^{2+}+Mg^{2+}+K^{+}+H+Al$; sum of bases ($SB=Ca^{2+}+Mg^{2+}+K^{+}$); Al^{3+} saturation on CEC1 ($m=Al^{3+}/CEC1\times100$); and base saturation percentage (BSP) ($BSP=SB/CEC2\times100$). P-rem is used in Brazil as a supplementary attribute to assess P buffering capacity (Rogeri et al., 2016), being affected by both soil texture and clay mineralogy. The P-rem was determined via molybdenum blue colorimetry after reaction of 10 g of sample in 100 mL of 60 mg L^{-1} P solution (Alvarez V. et al., 1999). S was extracted using 2 mol L^{-1} monocalcium phosphate in acetic acid solution and determination via spectrophotometry at 420 nm (Alvarez V. et al., 1999). B was determined by hot water extraction (Berger & Truog, 1939).

pXRF measurements

pXRF analyses were performed as established by USEPA Method 6200 (USEPA, 2007) and Weindorf and Chakraborty (2016), with minor modifications. Briefly, alluvial mud and soil sub-samples were sieved past 2-mm and oven-dried at 60°C for 2 weeks, then placed into sample cups retained by Mylar® thin-film at the bottom. The cups were placed on the pXRF aperture and scanned using an S1 Titan 600 LE in *Geochem–Dual soil* mode (Bruker, Billerica, MA, USA). The spectrometer contains a Rh tube (4 W, 15–50 keV and 5–100 μA) and a silicon drift detector with a resolution of < 145 eV. Each field sample was divided in two samples, and each one was analyzed in triplicate, totaling six measurements per field sample. The detection limits reported by the manufacturer are the following: Al and Si (0.4 g kg^{-1}); P and Cl (50 mg kg^{-1}); K, Ca, Ti, and V (25 mg kg^{-1}); Cr (10 mg kg^{-1}); Mn, Fe, Ni, Cu, Zn, As, Rb, Sr, Y, Zr, Ba, Ta, Pb, Bi, Ce (5 mg kg^{-1}). For quality assurance and quality control (QA/QC), blank samples, Bruker check-samples, and National Institute of Standards and Technology (NIST) certified reference materials (2709a, 2710a, and 2711a) were used to determine elemental recovery [(pXRF reported concentration/certified concentration)×100] (Silva et al., 2021). Bruker check-sample recoveries (%) were as follows: Al_2O_3 (97), K_2O (90); SiO_2 (94); Cu (98); Fe (90); Mn (89); Ni (102); Pb (100). The recoveries (%) for NIST standards were: Al_2O_3 (108); CaO (115); K_2O (80); SiO_2 (95); As (99); Ba (65); Cr (95); Cu (96); Fe (73); Mn (71); Ni (75); Pb (113); Rb (94); Sr (106); Ti (96); Zn (92); Zr (104).

Statistical analysis

Principal component analysis (PCA) using the "vegan" package in R (version 3.4.4) (R Development Core Team, 2019) with both pXRF and conventional laboratory soil data was performed to visualize differences between the sampling *sites* from the *Gualaxo*, *Carmo*, and *Doce* river sections. From the PCA results, comparisons between alluvial mud and soil were performed sequentially (see the "Exploratory analyses: differentiating river sections and sampling sites" section). Box-plot and descriptive statistics (minimum, maximum, mean, median, and standard deviation) were performed for both alluvial mud (*site* 1 + *site* 2) and soil (*site* 3) using pXRF and conventional laboratory results. Random forest (RF) regression, an ensemble learning technique, was used to predict conventional soil properties via pXRF data using pooled soil and alluvial mud samples (Breiman, 2001). In general, the RF algorithm combines numerous prediction trees where each tree is built from a bootstrap sample drawn from the calibration set. Notably, at each node of the tree the candidate set of the predictor is a random subset of all the predictors. The final prediction of a new observation is calculated as the average of the predictions from all the trees in the forest. Researchers have established that the RF ensemble shows better prediction than an individual tree. In this study, the "randomforest" package in R (version 3.4.4) (R Development Core Team, 2019) was used to execute the RF model with 500 trees

(Breiman, 2001; Liaw & Wiener, 2002). The prediction accuracy was determined using the coefficient of determination (R^2). For executing the RF models, instead of splitting the data into calibration and validation sets, out-of-bag (OOB) prediction (similar to cross-validation) was employed (James et al., 2013).

Results and discussion

Exploratory analyses: differentiating river sections and sampling sites

Figures 2a, b show the output of the PCA analysis using pXRF and soil chemistry data, respectively. In Fig. 2a, PC1 and PC2 explained 53% of the samples' variability. Mud (impacted area) and native soils (non-impacted area) were clearly differentiated, with little overlapping at 95% of confidence. However, no distinction could be made between mud samples with or without emergency interventions (site 1 *vs.* site 2). Furthermore, there were no clear differences between river sections (*Gualaxo*, *Carmo*, and *Doce*).

Alluvial mud was mostly associated to Fe, Cr, and SiO_2, while soils were more correlated with Al_2O_3, Ti, Zr, and Zn (Fig. 2a). Fe was the variable most influential on mud samples. Guerra et al. (2017) previously demonstrated that due to the high Fe concentration in the mud, the Fe peak obtained in the X-ray spectrum creates a clear distinction between deposited alluvial mud and surrounding soils, which parallels our results. Using fertility data, the two first principal components (PC1 and PC2) explained 60% of the samples' variability (Fig. 2b). Similar to what was observed with pXRF data, mud and soil groups were apparent, but no distinction could be made between mud samples with or without emergency interventions (*site* 1 *vs. site* 2). Conversely, a slightly better grouping of soils from each river area could be observed. The pH, BSP, available-P and Mn, and P-rem were the factors most correlated with alluvial mud, while Al^{3+}, SOM, H + Al, Al saturation (m), and CEC2 were positively correlated with soil samples. Based on the PCA results, it was irrelevant to separate emergency intervention from nonintervention areas (sites 1 and 2, respectively) in the alluvial mud samples. Therefore, hereafter, intervention and nonintervention samples were combined into a single category (mud), and the comparisons are presented between mud and native soils only.

Soil fertility

Soil and mud fertility properties are presented in Fig. 3; the complete soil fertility analyses with

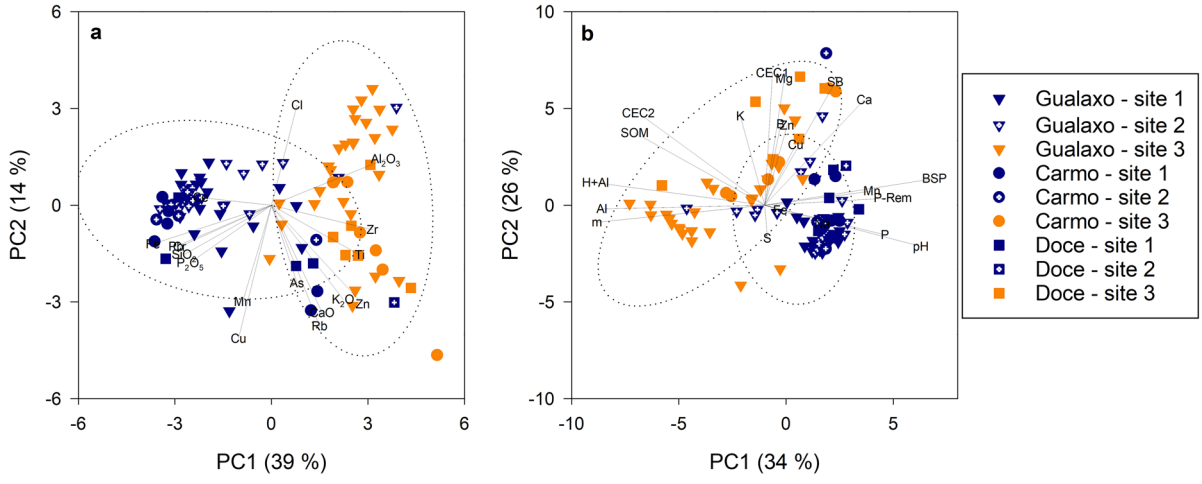

Fig. 2 River sections and sampling site differentiation based on principal component analysis (PCA) using data obtained with portable X-ray fluorescence (pXRF) (**a**) and conventional soil fertility (**b**) analyses. Rivers: *Gualaxo*, *Carmo*, and *Doce*. *Site* 1—mud deposition with emergency actions; *Site* 2—mud deposition with no emergency actions; and *Site* 3—native surrounding soils. Confidence ellipses were created at 95% of probability. The position of the different variables represents their PCA score

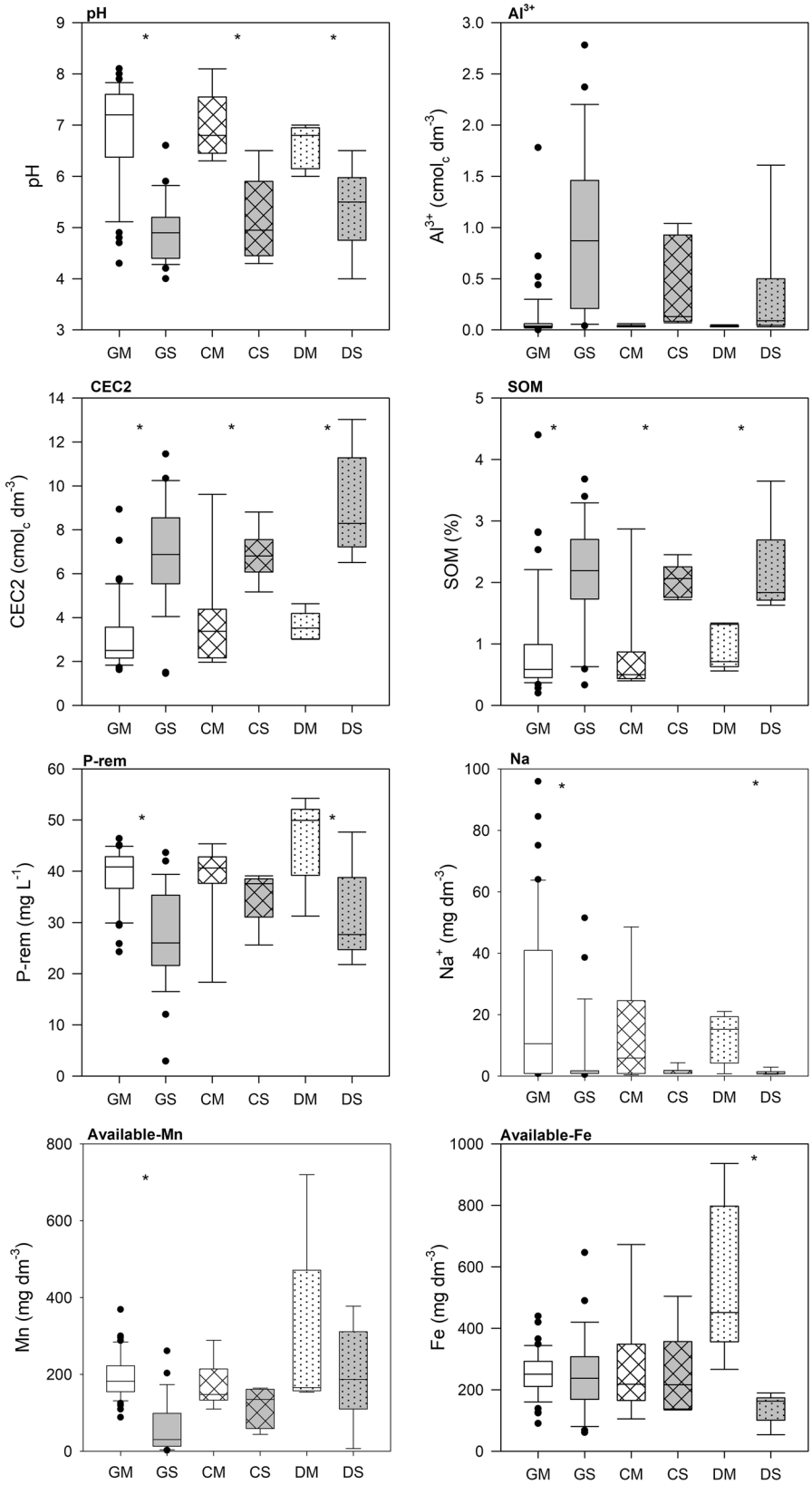

Fig. 3 Box-plot of alluvial mud (white) and native soils (gray) fertility properties obtained via conventional soil analysis across the three different river sections (*Gualaxo*, *Carmo*, and *Doce*). GM: *Gualaxo*–mud; GS: *Gualaxo*–soil; CM: *Carmo*–mud; CS: *Carmo*–soil; DM: *Doce*–mud; DS: *Doce*–soil. *Significant differences between mud and native soils at $\alpha = 0.05$ (Student's *t* test)

descriptive statistics are presented in Supplemental Table S1. The mean pH values of alluvial mud were higher than those of soil (Fig. 3). Mud pH values ranged from 4.30 to 8.10 while soil pH ranged from 4.00 to 6.60. In the impacted area, 70% of mud samples had pH >6.5 (Supplemental Table S1). In previous studies, mud pH ranged from 5.69 (Schaefer et al., 2016) to 8.24 (Silva et al., 2016), which corroborates with our findings. The alkaline values found for mud samples are mostly related to the Fe concentration process which employs chemicals (e.g., sodium hydroxide) to increase the pH and reach the point of zero charge (maximum flocculation) of Fe-oxides (Almeida et al., 2018). Given the high concentration of iron oxides in the mud (Fig. 4) and overall mud mineralogy (e.g., quartz, hematite and goethite, with smaller amounts of illite, kaolinite, muscovite; Almeida et al., 2018; Silva et al., 2016), its reactivity is pH-dependent. The higher mud pH can have implications for metallic micronutrient and contaminant dynamics and availability compared to native soils (Duarte et al., 2021; Queiroz et al., 2018; Zago et al., 2019). Similarly, pH has also been reported to drive microbial traits in impacted areas (Batista et al., 2020). The wider pH range observed in mud relative to native soils may reflect two distinct processes: (1) alluvial mud and mixed sediments carried downstream being heterogeneously deposited and distributed across river margins, and (2) a progressive acidification over time due to plant establishment and organic acid release.

In line with the Fe concentration processes, mud Na^+ concentrations were higher (4.4-fold) compared with Na^+ in the soil (Fig. 3). The mean Na^+ concentration (19.45 mg dm^{-3}) in mud was almost two times higher than that reported by Schaefer et al. (2016) but is in the lower range reported by Santos et al. (2019) across the impacted area. These highly variable results suggest a nonhomogeneous deposition and distribution of Na^+ and reinforce the need for constant monitoring and a detailed sampling scheme to generate accurate mapping and allow for effective remediation actions. Na^+ is not an essential element either for growth and development or for reproduction of almost all terrestrial plants, but high Na^+ concentrations may have deleterious effects on growth of non-salt tolerant plants (Maathuis, 2014). In the present study, Na^+ saturation on CEC2 or Na^+ absorption ratio (the relative concentration of Na^+, Ca^{2+}, and Mg^{2+}) were still considered low, but a few samples exhibited higher values (>5%) that could indicate potential soil structural degradation and plant toxicity (Gupta & Abrol, 1990).

The sum of bases ($Ca^{2+} + Mg^{2+} + K^+$), CEC1, and CEC2 of mud were lower than the soil (Fig. 3; Supplemental Table S1). Compared to native soil, mud had lower K^+ and Mg^{2+}, and higher concentrations of Na^+, Ca^{2+}, and P. In both cases, the concentrations of P, K^+, Ca^{2+}, and Mg^{2+} for both mud and soil were low/very low for plant growth (Alvarez V. et al., 1999). Considering the extraction process, it is unlikely that the mud itself would yield higher concentrations for P and Ca than the soil. This may be a result of emergency actions adopted in the impacted area, for instance, manure or P-fertilizer application (Renova, 2018). Although a thorough separation of the sampling locations was attempted (site 1 *vs.* site 2), emergency actions immediately following the breach were rushed, hampering a rigorous control. Thus, it is likely that a few areas that were still covered by native vegetation (site 2; Fig. 1) also received some intervention.

The SOM in mud was lower than soil and similar to the SOM concentrations reported in previous studies in the area (Fig. 3) (Schaefer et al., 2016; Silva et al., 2016). Increasing organic matter in mud-affected soils is an effective strategy for phyto-management and area remediation and should be a priority. Zago et al. (2019) reported that plants grown in the tailing substrates amended with organic compost were able to exclude potentially hazardous substances and therefore increase their tolerance to adverse environmental conditions. The concentration of available micronutrients (Zn, Fe, Cu, B) in mud and soil were similar (Fig. 3; Supplemental Table S1). However, available Mn concentrations were ~2-fold higher in mud samples compared with native soil. This result parallels other studies which reported higher Mn assimilation in plants grown on tailing substrates compared with plants grown on control soils (Coelho et al., 2020; Zago et al., 2019). Redox conditions in the impacted area favor the reduction of Mn-oxides to available and soluble forms ($Mn^{4+} \rightarrow Mn^{2+}$) (Sparrow & Uren, 2014), and thus favor plant uptake. Moreover, increasing Mn availability over time with subsequent dissolution in river water may pose a chronic risk of estuary contamination, with harmful

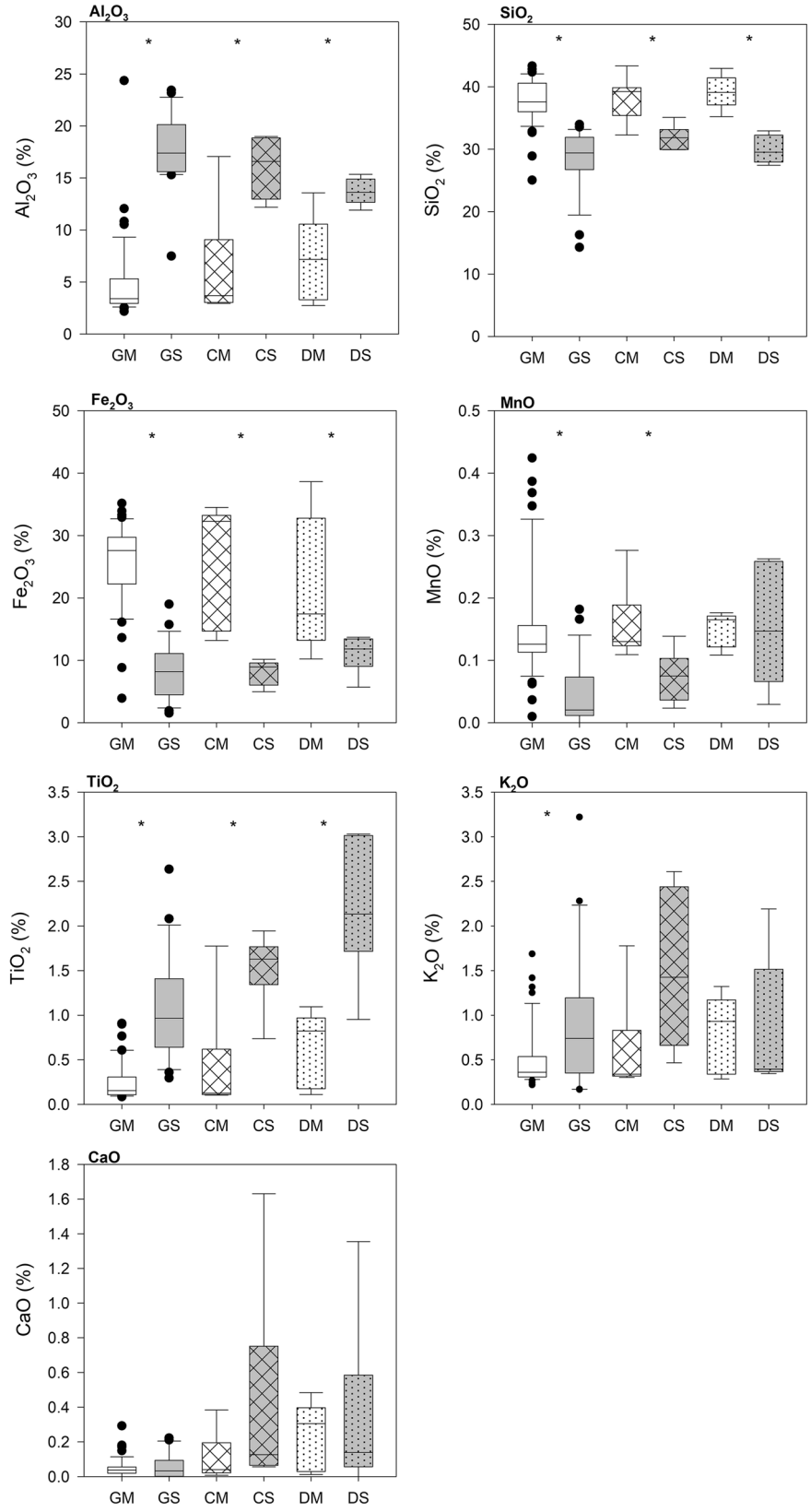

Fig. 4 Box-plot of major compounds of alluvial mud (white) and native soils (gray) obtained via portable X-ray fluorescence (pXRF) spectrometry across the three different river sections (*Gualaxo*, *Carmo*, and *Doce*). GM: *Gualaxo*–mud; GS: *Gualaxo*–soil; CM: *Carmo*–mud; CS: *Carmo*–soil; DM: *Doce*–mud; DS: *Doce*–soil. *Significant differences between mud and native soils at $\alpha = 0.05$ (Student's *t* test)

consequences for estuarine biota and human health (Queiroz et al., 2021).

pXRF data

For both alluvial mud and soil samples, the major constituents were SiO_2, Fe_2O_3, Al_2O_3, K_2O, and TiO_2 (Fig. 4; Table 1), reflecting mineralogy of mud and native soils as determined in previous studies; mostly quartz, hematite and goethite, and gibbsite with smaller amounts of illite, kaolinite, muscovite, and maghemite also observed (Almeida et al., 2018; Duarte et al., 2021; Silva et al., 2016). For all river sections, mud was richer than soil in SiO_2, Fe_2O_3, and MnO (Fig. 4). The prevalence of Si and Fe oxides in the mud reflects the expected composition of mining wastes as a result of exploration for itabirite (quartz and hematite) (Silva et al., 2016). The Fe concentration in mud was 2.7-fold that of soil. The soil contained higher concentrations of Al_2O_3 (2.6-fold) and TiO_2 (3.7-fold) (Fig. 4). Fe, Si, and Al oxides together accounted for >50% of mud or soil composition (Table 1). The accumulation of Fe and Si oxides in alluvial mud, and the reduction of Al oxide concentrations, indicate a distinct composition between mud and native soils. The confidence intervals showed that concentrations were fairly constant for mud and soil through the different river sections. However, an exception was observed for TiO_2, which showed greater values in the *Doce* compared with other river sections. Notably, the number of samples in the *Doce* river was smaller than in other sections due to the distance from the accident, section length, and damming (Fig. 1), which hamper spatial comparisons. No significant difference between mud and soil was observed for CaO and K_2O.

Table 1 Descriptive statistics of alluvial mud and native soil total elemental concentration obtained with portable X-ray fluorescence (pXRF) in riparian areas impacted by the *Fundão* dam collapse

	Minimum		Maximum		Median		Average		SD	
	Mud	Soil	Mud	Soil	Mud	Soil	Mud	Soil	Mud	Soil
SiO_2 (g kg^{-1})	250	143	433	369	381	299	379	297	35	45
Fe_2O_3 (g kg^{-1})	39	15	386	190	276	86	255	86	74	40
Al_2O_3 (g kg^{-1})	22	66	244	234	35	161	54	164	40	37
K_2O (g kg^{-1})	2	2	18	32	4	7	5	10	4	8
TiO_2 (g kg^{-1})	0.83	2.94	17.76	30.32	1.58	13.61	3.04	13.44	3.19	7.31
MnO (g kg^{-1})	0.10	---	14.04	2.63	1.30	0.54	1.71	0.69	1.80	0.71
Ce (mg kg^{-1})	---	---	2,019	2,478	1,545	1,168	1,393	909	503	696
P_2O_5 (mg kg^{-1})	---	---	1,582	2,431	1,259	719	1,185	703	299	459
Cl (mg kg^{-1})	144	372	940	1,025	662	668	629	683	162	150
CaO (mg kg^{-1})	---	---	4,838	16,307	398	683	736	1,687	1,004	3,309
Cr (mg kg^{-1})	---	---	385	736	248	47	231	99	83	144
Pb (mg kg^{-1})	---	---	135	78	53	26	52	22	26	20
Zr (mg kg^{-1})	14	68	382	407	29	168	60	183	71	70
Cu (mg kg^{-1})	2	3	79	58	27	19	27	22	9	14
Rb (mg kg^{-1})	13	---	95	167	22	27	26	40	14	41
Bi (mg kg^{-1})	---	---	69	---	14	---	18	---	19	---
Zn (mg kg^{-1})	---	13	55	81	14	30	16	33	11	16
Y (mg kg^{-1})	---	---	---	117	---	14	---	17	---	22
V (mg kg^{-1})	---	---	---	---	---	---	---	---	---	---
Ta (mg kg^{-1})	---	---	---	---	---	---	---	---	---	---
Sr (mg kg^{-1})	---	---	---	151	---	13	---	28	---	35
Ni (mg kg^{-1})	---	---	---	208	---	18	---	34	---	48
Ba (mg kg^{-1})	---	---	---	---	---	---	---	---	---	---
As (mg kg^{-1})	---	---	---	---	---	---	---	---	---	---

--- means not detected or below equipment detection limit. Percentage of elements not detected in the mud samples (Y, 75%; V, 97%; Ta, 98%; Sr, 78%; Ni, 88%; Ba, 78%; As, 92%). Percentage of elements not detected in the soil samples (Bi, 61%; V, 51%; Ta, 62%; Ni, 38%; Ba, 67%; As, 84%)

sd standard deviation

Assessing hazardous elements via pXRF

The values reported by pXRF in Table 1 represent the total elemental composition. Although pXRF is not an official method for assessing soil contamination in Brazil (e.g., mining areas), Kilbride et al. (2006) found a strong correlation between pXRF and aqua regia digestion followed by ICP-OES quantification for Cu, Pb, As, Cd, Zn, Fe, Ni, and Mn. Also, Wallis and Walker (1999) demonstrated that pXRF was very accurate for determining As and Pb concentrations in mining areas. In Brazil, contamination assessment of soils and sediments is based on semi-total threshold values established by the National Environmental Council (Conama Resolution, 420/2009). The following elements are regulated based on semi-total concentration: As, Ba, B, Co, Cd, Cr, Cu, Hg, Mo, Ni, Pb, Sb, and Zn (Conama Resolution, 420/2009). From this list, only As, Cu, Cr, Ni, Pb, and Zn were detected via pXRF (Table 1). The assessment of contamination levels of these hazardous pollutant elements with pXRF is not possible since soil quality reference threshold values were established based on semi-total concentrations (Conama Resolution, 420/2009). With this constraint, whenever presented, semi-total reference values are simply to put data in a broad perspective. Comparisons performed in this section are most valid when comparing pXRF data of alluvial mud vs. native soil. Nevertheless, it should be stressed that total concentration lesser than established semi-total threshold values indicate that bioavailable forms should be even lower in an environmental risk assessment framework.

Most studies conducted in the impacted area by the Mariana dam disaster suggest that the alluvial mud is not a significant source of hazardous heavy metals (Davila et al., 2020; Guerra et al., 2017; Silva et al., 2016). In some instances, the heavy metal concentrations in surrounding soils were higher than those found in mud (Davila et al., 2020). However, other studies have found an increase in potentially hazardous heavy metal concentrations after the dam collapse (Duarte et al., 2021). In our study, the mean total concentration of Cr in the mud samples was 231 mg kg^{-1}, which was higher than the level observed in surrounding soils (99 mg kg^{-1}). The Cr enrichment observed is possibly a result of the alluvial mud and river sediments mixed downstream (Duarte et al., 2021). The *Doce* river basin has been reported to have a naturally higher Cr concentration than other regions of Minas Gerais state (281 mg kg^{-1}; Guevara et al., 2018). For Pb, the obtained mean value (52 mg kg^{-1}) was lower than the established semi-total soil quality reference threshold value (72 mg kg^{-1}; Conama Resolution, 420/2009). However, the mean Pb concentration in the alluvial mud was 2.4 times higher than that obtained in surrounding soils, and concentrations up to 135 mg kg^{-1} were found (Table 1). Mean As concentration for mud and soil samples was 22.7 ($\pm$11.7) mg kg^{-1}. However, this element was not detected in 92% and 84% of mud and soil samples, respectively. Contrariwise, Duarte et al. (2021) indicated that As sources were present in the area before the disaster and As concentration increased in the area due to sediment remobilization.

Regardless of bulk or semi-total concentrations reported here and elsewhere (Almeida et al., 2018; Davila et al., 2020; Duarte et al., 2021; Guerra et al., 2017; Queiroz et al., 2018), most studies performed in the region confirm the high heterogeneity of the material deposited on river margins and its distinct composition when compared with surrounding soils. The occurrence of hazardous elements in alluvial mud raises concern since seasonal flooding can cause variations in the pH and redox conditions, which directly influences metal availability (Queiroz et al., 2018). Moreover, the distinct chemical composition of alluvial mud and soils (Figs. 2 and 4; Table 1) suggest that element dynamics can be uncertain. Therefore, while heavy metal concentrations can be low overall, the potential availability of hazardous pollutants in the impacted area implies thorough investigations and constant monitoring are needed to establish a safe new scenario for crop-livestock-forest production over impacted areas (Andrade et al., 2018; Fernandes et al., 2016).

Prediction of soil fertility properties using pXRF

In this study, RF regression was used to correlate pXRF variables with conventional laboratory analysis and predict fertility properties in mud and soil samples (Figs. 5, 6, 7, and 8). Notably, pXRF produced significant pH prediction accuracy (Fig. 5) in the pooled dataset (OOB $R^2 = 0.80$). Moderate prediction performance was achieved for CEC1 (OOB $R^2 = 0.52$), CEC2 (OOB $R^2 = 0.53$), and SOM (OOB $R^2 = 0.54$). Additionally, RF yielded

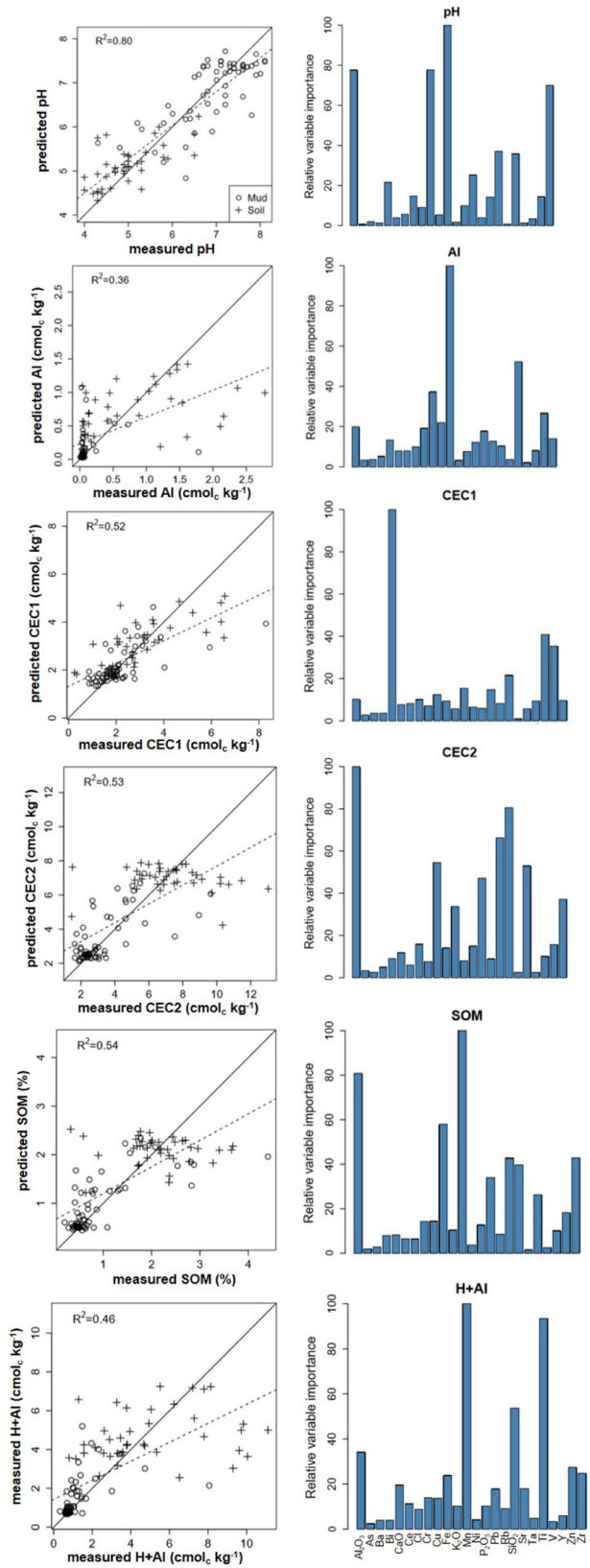

Fig. 5 Random forest prediction of pH, exchangeable Al, effective cation exchange capacity (CEC1), potential exchange capacity at pH 7.0 (CEC2), soil organic matter (SOM), and H + Al using portable X-ray fluorescence (pXRF) data for pooled mud and soil samples

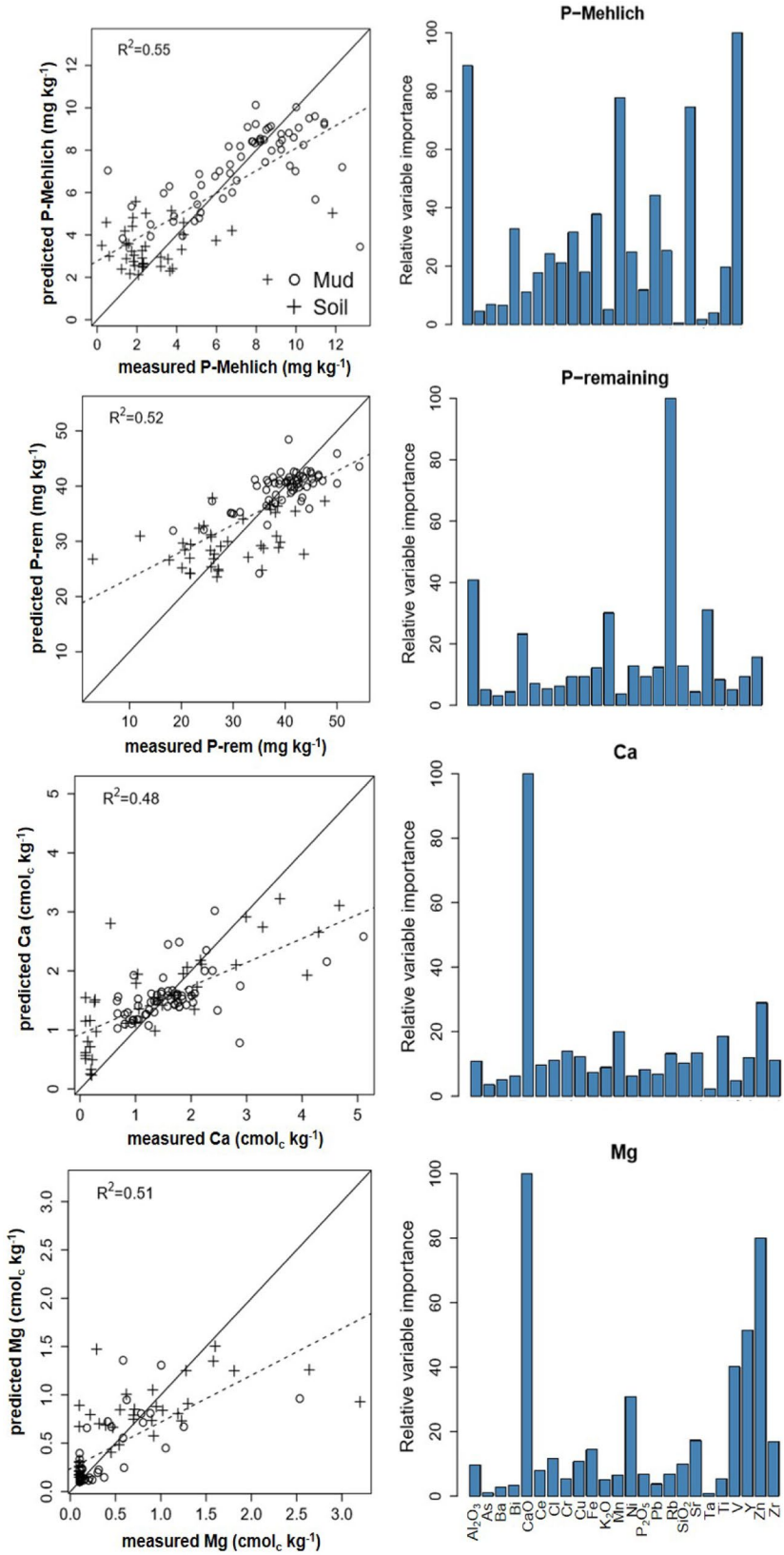

Fig. 6 Random forest prediction of available P (P-Mehlich), P-remaining (P-rem), and exchangeable Ca^{2+} and Mg^{2+} using portable X-ray fluorescence (pXRF) data for pooled mud and soil samples

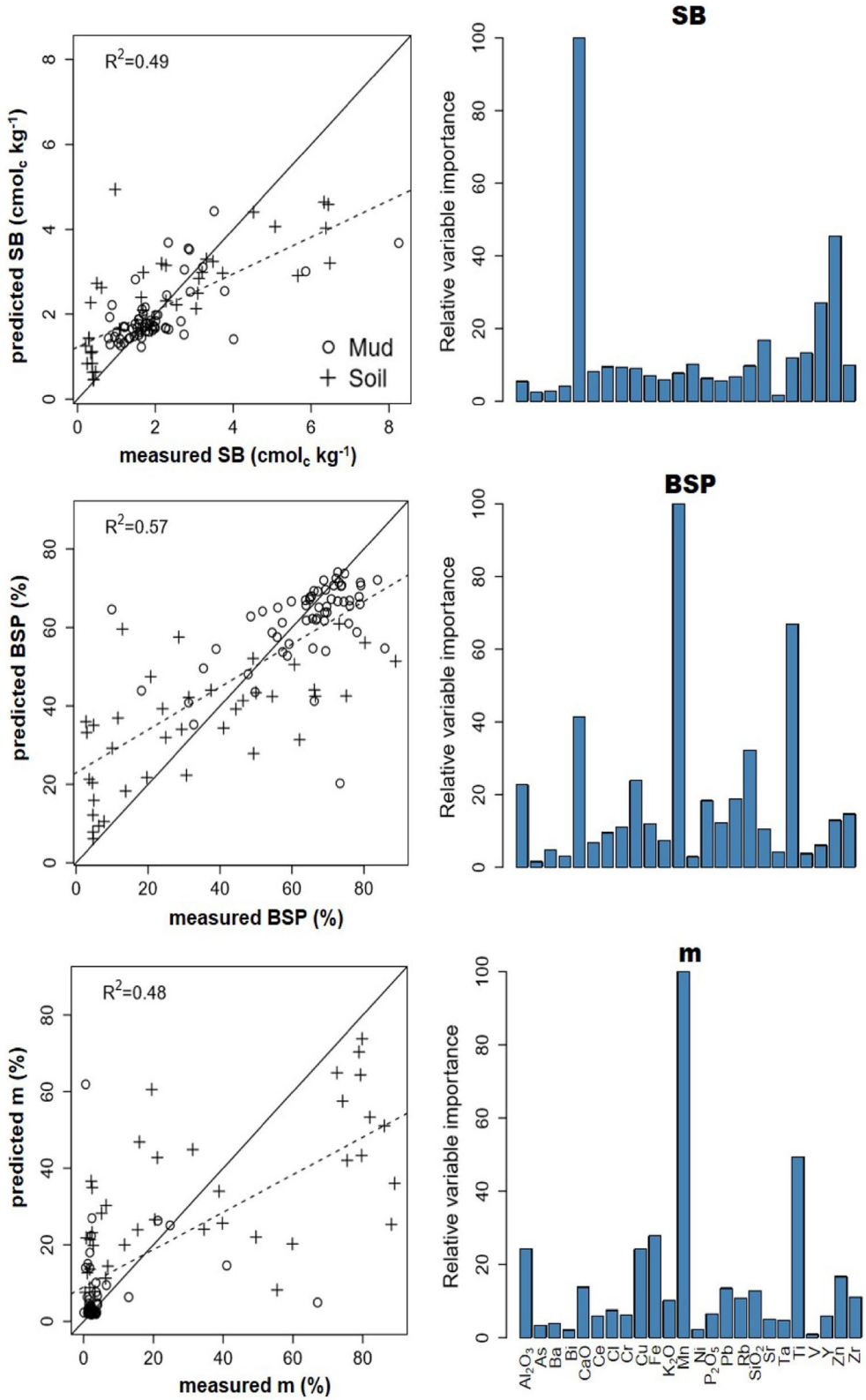
R²=0.49
predicted SB (cmol_c kg⁻¹)
measured SB (cmol_c kg⁻¹)
Mud
Soil
SB
Relative variable importance
R²=0.57
predicted BSP (%)
measured BSP (%)
BSP
Relative variable importance
R²=0.48
predicted m (%)
measured m (%)
m
Relative variable importance
Al2O3
As
Ba
Bi
CaO
Ce
Cl
Cr
Cu
Fe
K2O
Mn
Ni
P2O5
Pb
Rb
SiO2
Sr
Ta
Ti
V
Y
Zn
Zr

◂ **Fig. 7** Random forest prediction of sum of bases (SB), base saturation percentage (%), and Al-saturation on CEC1 (m) (%) using portable X-ray fluorescence (pXRF) data for pooled mud and soil samples

moderate prediction accuracy for P-Mehlich (OOB $R^2 = 0.55$), P-rem (OOB $R^2 = 0.52$), available Ca and Mg (OOB $R^2 = 0.48$ and 0.51, respectively) (Fig. 6), SB (OOB $R^2 = 0.49$), BSP (OOB $R^2 = 0.57$), m (OOB $R^2 = 0.48$) (Fig. 7), and available Mn (OOB $R^2 = 0.50$) (Fig. 8). Surprisingly, RF could not produce high prediction accuracy for available Fe (OOB $R^2 = 0.24$), Zn (OOB $R^2 = 0.39$), and Cu (OOB $R^2 = 0.40$) (Fig. 8). The prediction performance worsened for exchangeable Al (OOB $R^2 = 0.36$) and H + Al (OOB $R^2 = 0.46$) due to a few samples with higher concentrations.

The ability of pXRF to predict soil pH was demonstrated earlier by Sharma et al. (2014). However, the prediction accuracy for CEC1 obtained in our study ($R^2 = 0.52$) was lower than observed in Sharma et al. (2015), which exhibited higher prediction accuracy ($R^2 = 0.91$) for soil CEC1 using pXRF elemental data. Nevertheless, most predictions are reasonable since they were performed with the pooled samples (mud and soil), which consist of two chemically distinct matrices (Fig. 2). After the dam rupture, the relatively homogeneous mud (Silva et al., 2016) was mixed downstream with several other materials (e.g., vegetation, native soils, river sediments, and slurry tanks). This resulted in a highly heterogeneous material but without data and spatial distribution to allow an accurate prediction of soil fertility properties. An alternative to increase accuracy would be to generate prediction models for mud or native soils separately. However, this would require a much higher sampling intensity. In this initial screening, using pXRF was shown to be a feasible and practical tool for determining soil properties as a guide to establishing fertility management programs in the impacted areas. The results presented substantiate the conclusions made by Teixeira et al. (2020) where pXRF achieved reasonable predictions for soil pH, SB, CEC, BSP, and m for multiple Brazilian soils, while expanding pXRF applicability to pooled heterogeneous mixed matrices (native soil + mud + river sediments).

The RF variable importance plots showed the influence of Al_2O_3 and K_2O for predicting pH (Fig. 5). Indeed, other studies also have shown the influence of Al_2O_3 and K_2O for predicting soil pH (Sharma et al., 2014). Notably, Al_2O_3 also appeared influential for predicting SOM and CEC2 (Fig. 5). The influence of Al_2O_3 for predicting several soil properties can be attributed to the fact that it was one of the major compounds found in mud and soil samples—being higher in native soils (Fig. 2a; Fig. 4). Al_2O_3 is present in the crystalline structure of kaolinite and gibbsite, which are commonly found in Brazilian soils (Teixeira et al., 2020), including soils of impacted area (Duarte et al., 2021), and influence multiple processes in tropical soils such as organic matter and nutrient retention (Souza et al., 2017). As expected P_2O_5, CaO, and Mn were crucial for predicting P-Mehlich (Fig. 6), exchangeable Ca (Fig. 6), and available Mn (Fig. 8), respectively. CaO also appeared important for predicting SB in soil and mud samples (Fig. 7).

Conclusions

After the largest worldwide mining disaster, there is an urgent need for detailed characterization and constant monitoring of impacted areas to promote successful environmental rehabilitation. In this study, pXRF spectrometry was shown to be an effective method for providing rapid, environmentally friendly chemical characterization of impacted areas. Mud and native surrounding soils were clearly differentiated based on chemical signatures determined via pXRF (mainly SiO_2, Al_2O_3, Fe_2O_3, TiO_2, and MnO), in which mud was richer than soil in SiO_2, Fe_2O_3, and MnO, while native soils exhibited higher concentrations of Al_2O_3 and TiO_2 than mud. Regarding potential pollutant elements, the total concentrations of Cr and Pb were higher in the impacted area compared with surrounding native soils. Collectively, the distinct chemical composition and the potential presence of toxic elements suggest the need for continued monitoring to better understand the elemental dynamics and assess possible human and environmental risk through time.

Both pXRF data and random forest models successfully predicted pH regardless of substrate complexity (e.g., alluvial mud or native soil), which is most important as pH has direct implications for metallic nutrient and contaminant availability and mobility. Moderate predictions were obtained for

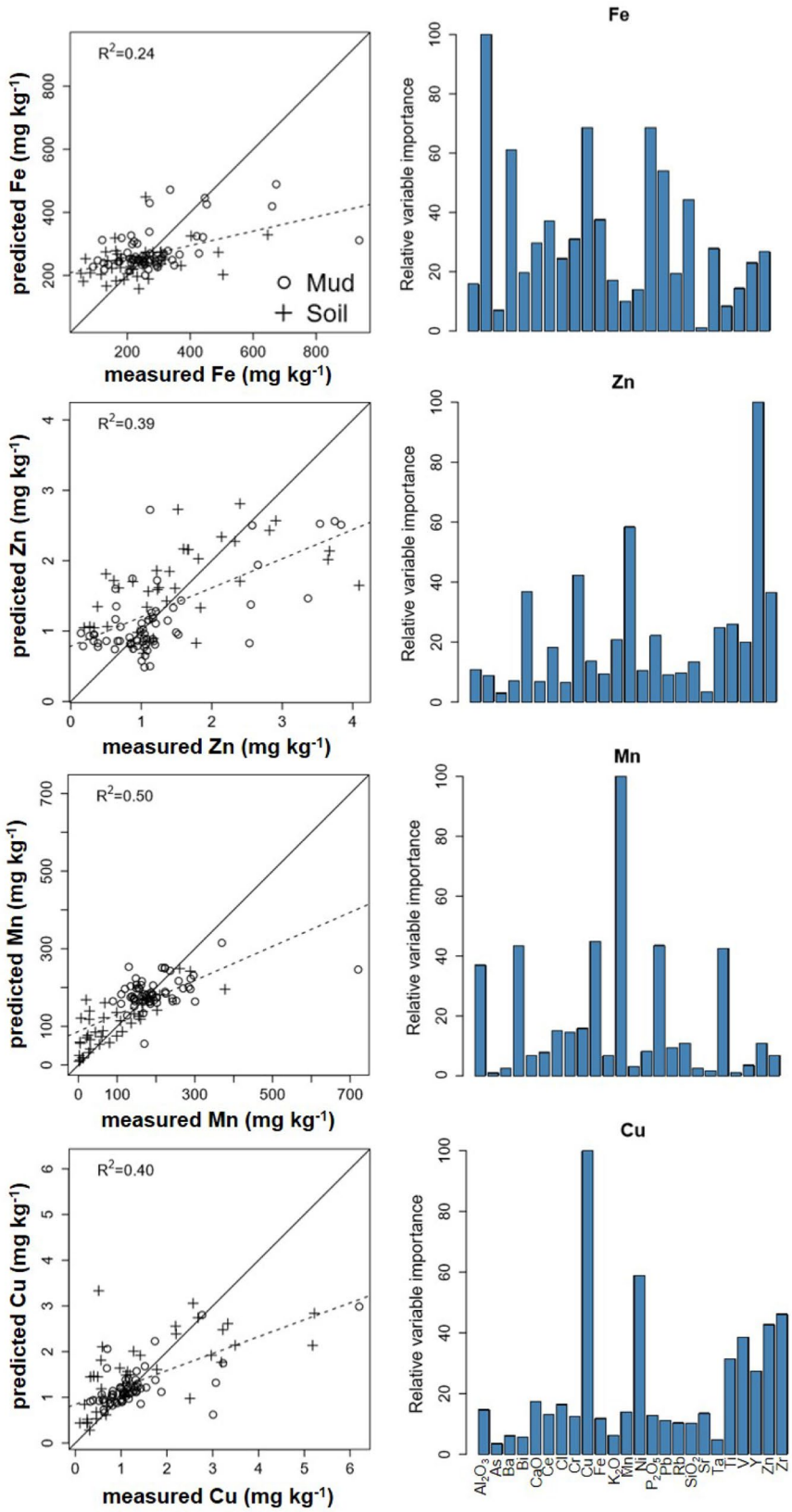

Fig. 8 Random forest prediction of available Fe, Zn, Mn, and Cu using portable X-ray fluorescence (pXRF) data for pooled mud and soil samples

SOM, CEC1, and CEC2, and available macro- and micronutrients, except for available Fe, Zn, and Cu. Results indicate that pXRF spectrometry can identify contamination hotspots, assess total elemental composition, differentiate alluvial mud from native soils, and reasonably predict related fertility properties. These findings demonstrate that the pXRF can be an important and rapid tool to intensify field sampling schemes with modest additional cost. Future efforts should use the pXRF in situ to substantially increase the practically of environmental monitoring.

Supplementary information The online version contains supplementary material available at https://doi.org/10.1007/s10661-021-08982-7.

Acknowledgements The authors thank Kalill V. Páscoa and Thiza F. Altoé for help with field work, and Geila S. Carvalho and Pedro E. D. Barbosa for assistance with pXRF spectra collection. The authors are grateful to Fundação Renova and landowners for field site access. In conducting this research, G.W.D.F thanks the Coordenação de Aperfeiçoamento de Pessoal de Nível Superior (CAPES) (process number 88887.144594/2017-00) for the scholarship during this study, B.T.R thanks the PrInt-Capes Program (process number 888887.363577/2019-00), and D.C.W. gratefully acknowledge the BL Allen Endowment in Pedology at Texas Tech University. We also thank three anonymous reviewers for constructive comments on an earlier manuscript version.

Funding This study was supported by the Fundação de Amparo à Pesquisa do Estado de Minas Gerais (FAPEMIG)—grant award number APQ-01733-16.

References

Abrahão, W. A. P., & Marques, J. J. (2013). *Manual de coleta de solos para valores de referência de qualidade no estado de Minas Gerais*. Belo Horizonte.

Aires, U. R. V., Santos, B. S. M., Coelho, C. D., da Silva, D. D., & Calijuri, M. L. (2018). Changes in land use and land cover as a result of the failure of a mining tailings dam in Mariana, MG, Brazil. *Land Use Policy, 70,* 63–70. https://doi.org/10.1016/j.landusepol.2017.10.026

Almeida, C. A., de Oliveira, A. F., Pacheco, A. A., Lopes, R. P., Neves, A. A., Ribeiro, L., & de Queiroz, M. E. (2018). Characterization and evaluation of sorption potential of the iron mine waste after Samarco dam disaster in Doce River basin – Brazil. *Chemosphere, 209,* 411–420. https://doi.org/10.1016/j.chemosphere.2018.06.071

Alvares, C. A., Stape, J. L., Sentelhas, P. C., Gonçalves, J. L. M., & Sparovek, G. (2013). Köppen's climate classification map for Brazil. *Meteorologische Zeitschrift, 22*(6), 711–728. https://doi.org/10.1127/0941-2948/2013/0507

Alvarez V. V. H., de Novais, R. F., de Barros, N. F., Cantarutti, R. B., & Lopes, A. S. (1999). Interpretação dos resultados das análises de solos. In A. C. Ribeiro, P. T. G. Guimarães, & V. H. Alvarez V. (Eds.), *Recomendações Para o Uso de Corretivos e Fertilizantes Em Minas Gerais - 5° Aproximação* (pp. 25–32). Viçosa, MG: Comissão de Fertilidade do Solo do Estado de Minas Gerais.

Andrade, G. F., Paniz, F. P., Martins, A. C., Rocha, B. A., da Silva Lobato, A. K., Rodrigues, J. L., et al. (2018). Agricultural use of Samarco's spilled mud assessed by rice cultivation: A promising residue use? *Chemosphere, 193,* 892–902. https://doi.org/10.1016/j.chemosphere.2017.11.099

Andrade, R., Faria, W. M., Silva, S. H. G., Chakraborty, S., Weindorf, D. C., Mesquita, L. F., et al. (2020). Prediction of soil fertility via portable X-ray fluorescence (pXRF) spectrometry and soil texture in the Brazilian Coastal Plains. *Geoderma, 357,* 113960. https://doi.org/10.1016/j.geoderma.2019.113960

Batista, É. R., Carneiro, J. J., Araújo Pinto, F., dos Santos, J. V., & Carneiro, M. A. C. (2020). Environmental drivers of shifts on microbial traits in sites disturbed by a large-scale tailing dam collapse. *Science of the Total Environment, 738,* 139453. https://doi.org/10.1016/j.scitotenv.2020.139453

Berger, K. C., & Truog, E. (1939). Boron determination in soils and plants using the quinalizarin reaction. *Industrial and Engineering Chemistry - Analytical Edition, 11*(10), 540–545. https://doi.org/10.1021/ac50138a007

Breiman, L. (2001). Random forests. *Machine Learning, 45,* 5–32. https://doi.org/10.1023/A:1010933404324

Coelho, D. G., Marinato, C. S., de Matos, L. P., de Andrade, H. M., da Silva, V. M., Neves, P. H. S., & de Oliveira, J. A. (2020). Evaluation of metals in soil and tissues of economic-interest plants grown in sites affected by the Fundão Dam failure in Mariana. *Brazil. Integrated Environmental Assessment and Management, 16*(5), 596–607. https://doi.org/10.1002/ieam.4253

Conselho Nacional do Meio Ambiente - Conama. (2009). Resolução Conama n° 420, de 28 de dezembro de 2009: Dispõe sobre critérios e valores orientadores de qualidade do solo quanto à presença de substâncias químicas e estabelece diretrizes para o gerenciamento ambiental de áreas contaminadas por essas substâncias em decorrência de atividades antrópicas [internet]. Brasília, DF. Available online at: http://www.mma.gov.br/port/conama/res/res09/res42009.pdf

Carmo, F. F., Kamino, L. H. Y., Junior, R. T., de Campos, I. C., do Carmo, F. F., Silvino, G., et al. (2017). Fundão tailings dam failures: the environment tragedy of the largest technological disaster of Brazilian mining in global context. *Perspectives in Ecology and Conservation, 15*(3), 145–151. https://doi.org/10.1016/j.pecon.2017.06.002

Davila, R. B., Fontes, M. P. F., Pacheco, A. A., & da Silva Ferreira, M. (2020). Heavy metals in iron ore tailings and floodplain soils affected by the Samarco dam collapse in Brazil. *Science of The Total Environment, 709,* 136151. https://doi.org/10.1016/j.scitotenv.2019.136151

Duarte, E. B., Neves, M. A., de Oliveira, F. B., Martins, M. E., de Oliveira, C. H. R., Burak, D. L., et al. (2021).

Trace metals in Rio Doce sediments before and after the collapse of the Fundão iron ore tailing dam, Southeastern Brazil. *Chemosphere*, *262*. https://doi.org/10.1016/j.chemosphere.2020.127879

Embrapa. (2011). *Manual de Métodos de Análise de Solo*. (G. K. Donagemma, Ed.) *Embrapa* (2nd ed.). Rio de Janeiro: Embrapa Solos. http://www.cnps.embrapa.br/publicacoes

Fernandes, G. W., Goulart, F. F., Ranieri, B. D., Coelho, M. S., Dales, K., Boesche, N., et al. (2016). Deep into the mud: ecological and socio-economic impacts of the dam breach in Mariana, Brazil. *Natureza e Conservacao, 14*(2), 35–45. https://doi.org/10.1016/j.ncon.2016.10.003

Gomes, L. E., Correa, L. B., Sá, F., Neto, R. R., & Bernardino, A. F. (2017). The impacts of the Samarco mine tailing spill on the Rio Doce estuary Eastern Brazil. *Marine Pollution Bulletin, 120*(1–2), 28–36. https://doi.org/10.1016/j.marpolbul.2017.04.056

Guerra, M. B. B., Teaney, B. T., Mount, B. J., Asunskis, D. J., Jordan, B. T., Barker, R. J., et al. (2017). Post-catastrophe analysis of the Fundão tailings dam failure in the Doce River system, southeast Brazil: Potentially toxic elements in affected soils. *Water, Air, and Soil Pollution, 228*(7), 1–12. https://doi.org/10.1007/s11270-017-3430-5

Guevara, Y. Z. C., De Souza, J. J. L. L., Veloso, G. V., Veloso, R. W., Rocha, P. A., Abrahão, W. A. P., & Filho, E. I. F. (2018). Reference values of soil quality for the Rio Doce Basin. *Revista Brasileira de Ciencia do Solo, 42,* 1–16. https://doi.org/10.1590/18069657rbcs20170231

Gupta, R. K., & Abrol, I. P. (1990). Salt-affected soils: their reclamation and management for crop production (pp. 223–288). https://doi.org/10.1007/978-1-4612-3322-0_7

Horta, A., Azevedo, L., Neves, J., Soares, A., & Pozza, L. (2021). Integrating portable X-ray fluorescence (pXRF) measurement uncertainty for accurate soil contamination mapping. *Geoderma*, *382*, 114712. https://doi.org/10.1016/j.geoderma.2020.114712

IUSS Working Group WRB. (2015). *World Reference Base for Soil Resources* 2014*, update* 2015 *International soil classification system for naming soils and creating legends for soil maps.* World Soil Reports. Rome, Italy: FAO. https://doi.org/10.1017/S0014479706394902

James, G., Witten, D., Hastie, T., & Tibshirani, R. (2013). *An Introduction to Statistical Learning* (Vol. 103). Springer, New York. https://doi.org/10.1007/978-1-4614-7138-7

Jang, M. (2010). Application of portable X-ray fluorescence (pXRF) for heavy metal analysis of soils in crop fields near abandoned mine sites. *Environmental Geochemistry and Health, 32*(3), 207–216. https://doi.org/10.1007/s10653-009-9276-z

Kilbride, C., Poole, J., & Hutchings, T. R. (2006). A comparison of Cu, Pb, As, Cd, Zn, Fe, Ni and Mn determined by acid extraction/ICP-OES and ex situ field portable X-ray fluorescence analyses. *Environmental Pollution, 143*(1), 16–23. https://doi.org/10.1016/j.envpol.2005.11.013

Liaw, A., & Wiener, M. (2002). Classification and regression by random forest. *R News*, *2/3*, 18–22.

Lima, T. M, Weindorf, D. C., Curi, N., Guilherme, L. R. G., Lana, R. M. Q., & Ribeiro, B. T. (2019). Elemental analysis of Cerrado agricultural soils via portable X-ray fluorescence spectrometry: Inferences for soil fertility assessment. *Geoderma*, *353*, 264–272. https://doi.org/10.1016/j.geoderma.2019.06.045

Maathuis, F. J. M. (2014). Sodium in plants: Perception, signalling, and regulation of sodium fluxes. *Journal of Experimental Botany, 65*(3), 849–858. https://doi.org/10.1093/jxb/ert326

Miranda, L. S., & Marques, A. C. (2016). Hidden impacts of the Samarco mining waste dam collapse to Brazilian marine fauna – an example from the staurozoans (Cnidaria). *Biota Neotropica, 16*(2), 1–3. https://doi.org/10.1590/1676-0611

Omachi, C. Y., Siani, S. M. O., Chagas, F. M., Mascagni, M. L., Cordeiro, M., Garcia, G. D., et al. (2018). Atlantic Forest loss caused by the world's largest tailing dam collapse (Fundão Dam, Mariana, Brazil). *Remote Sensing Applications: Society and Environment, 12*, 30–34. https://doi.org/10.1016/j.rsase.2018.08.003

Peinado, F. M., Ruano, S. M., González, M. G. B., & Molina, C. E. (2010). A rapid field procedure for screening trace elements in polluted soil using portable X-ray fluorescence (PXRF). *Geoderma, 159*(1–2), 76–82. https://doi.org/10.1016/j.geoderma.2010.06.019

Queiroz, H. M., Nóbrega, G. N., Ferreira, T. O., Almeida, L. S., Romero, T. B., Santaella, S. T., et al. (2018). The Samarco mine tailing disaster: A possible time-bomb for heavy metals contamination? *Science of the Total Environment, 637–638,* 498–506. https://doi.org/10.1016/j.scitotenv.2018.04.370

Queiroz, H. M., Ying, S. C., Abernathy, M., Barcellos, D., Gabriel, F. A., Otero, X. L., et al. (2021). Manganese: The overlooked contaminant in the world largest mine tailings dam collapse. *Environment International*, *146*. https://doi.org/10.1016/j.envint.2020.106284

R Development Core Team. (2019). *R: a language and environment for statistical computing*. R Foundation for Statistical Computing.

Renova, F. (2018). *Monitoramento das intervenções prioritárias: Relatório de resultado do primeiro ano de monitoramento*. Belo Horizonte, MG. https://www.fundacaorenova.org

Ribeiro, B. T., Silva, S. H. G., Silva, E. A., & Guilherme, L. R. G. (2017). Portable X-ray fluorescence (pXRF) applications in tropical Soil Science. *Ciência e Agrotecnologia, 41*(3), 245–254. https://doi.org/10.1590/1413-70542017413000117

Rogeri, D. A., Gianello, C., Bortolon, L., & Amorim, M. B. (2016). Substitution of clay content for P-remaining as an index of the phosphorus buffering capacity for soils of Rio Grande do Sul. *Revista Brasileira de Ciência do Solo, 40,* 1–14. https://doi.org/10.1590/18069657rbcs20140535

Rouillon, M., & Taylor, M. P. (2016). Can field portable X-ray fluorescence (pXRF) produce high quality data for application in environmental contamination research? *Environmental Pollution, 214,* 255–264. https://doi.org/10.1016/j.envpol.2016.03.055

Santos, O. S. H., Avellar, F. C., Alves, M., Trindade, R. C., Menezes, M. B., Ferreira, M. C., et al. (2019). Understanding the environmental impact of a mine dam rupture in Brazil: Prospects for remediation. *Journal of Environmental Quality, 48*(2), 439–449. https://doi.org/10.2134/jeq2018.04.0168

Santos Teixeira, A. F., Pelegrino, M. H. P., Faria, W. M., Silva, S. H. G., Gonçalves, M. G. M., Acerbi Júnior, F. W., et al. (2020). Tropical soil pH and sorption complex prediction via portable X-ray fluorescence spectrometry. *Geoderma, 361,* 114132. https://doi.org/10.1016/j.geoderma.2019.114132

Schaefer, C. E. G. R., Santos, E. E., Fernandes Filho, E. I., & Assis, I. R. (2016). Paisagens de lama: Os tecnossolos para recuperação ambiental de áreas afetadas pelo desastre da Barragem de Fundão, em Mariana. *Boletim Infromativo da SBCS, Jan-Abr, 42*(1), 18–23.

Schaefer, C. E. G. R., Santos, E. E., Souza, C. M., Damato Neto, J., Filho, E. I. F., & Delpupo, C. (2015). Cenário histórico, quadro físiográfico e estratégias para recuperação ambiental de Tecnossolos nas áreas afetadas pelo rompimento da barragem do Fundão, Mariana, MG. *Arquivos do Museu de História Natural e Jardim Botânico da UFMG*, *24*(1–2), 105–135. https://seer.ufmg.br/index.php/mhnjb/article/view/11332/8524

Segura, F. R., Nunes, E. A., Paniz, F. P., Paulelli, A. C. C., Rodrigues, G. B., Braga, G. Ú. L., et al. (2016). Potential risks of the residue from Samarco's mine dam burst (Bento Rodrigues, Brazil). *Environmental Pollution, 218,* 813–825. https://doi.org/10.1016/j.envpol.2016.08.005

Selmi, M., Lagoeiro, L. E., & Endo, I. (2009). Geochemistry of hematitite and itabirite, Quadrilátero Ferrífero, Brazil. *Rem: Revista Escola de Minas, 62*(1), 35–43. https://doi.org/10.1590/S0370-44672009000100006

Sharma, A., Weindorf, D. C., Man, T., Aldabaa, A. A. A., & Chakraborty, S. (2014). Characterizing soils via portable X-ray fluorescence spectrometer: 3. Soil reaction (pH). *Geoderma, 232–234,* 141–147. https://doi.org/10.1016/j.geoderma.2014.05.005

Sharma, A., Weindorf, D. C., Wang, D. D., & Chakraborty, S. (2015). Characterizing soils via portable X-ray fluorescence spectrometer: 4. Cation exchange capacity (CEC). *Geoderma, 239,* 130–134. https://doi.org/10.1016/j.geoderma.2014.10.001

Silva, A., Cavalcante, L., Fabris, J., Franco Junior, R., Barral, U., Farnezi, M., et al. (2016). Chemical, mineralogical and physical characteristics of a material accumulated on the river margin from mud flowing from the collapse of the iron ore tailings dam in Bento Rodruigues, Minas Gerais, Brazil. *Revista Espinhaço, 5*(2), 44–53.

Silva Junior, C. A., Coutinho, A. D., Oliveira-Júnior, J. F., Teodoro, P. E., Lima, M., Shakir, M., et al. (2018). Analysis of the impact on vegetation caused by abrupt deforestation via orbital sensor in the environmental disaster of Mariana Brazil. *Land Use Policy, 76*(March), 10–20. https://doi.org/10.1016/j.landusepol.2018.04.019

Silva, S. H. G., Ribeiro, B. T., Guerra, M. B. B., de Carvalho, H. W. P., Lopes, G., Carvalho, G. S., et al. (2021). pXRF in tropical soils: Methodology, applications, achievements and challenges. https://doi.org/10.1016/bs.agron.2020.12.001

Silva, S. H. G., Weindorf, D. C., Pinto, L. C., Faria, W. M., Acerbi Junior, F. W., Gomide, L. R., et al. (2020). Soil texture prediction in tropical soils: A portable X-ray fluorescence spectrometry approach. *Geoderma, 362,* 114136. https://doi.org/10.1016/j.geoderma.2019.114136

Souza, I. F., Archanjo, B. S., Hurtarte, L. C. C., Oliveros, M. E., Gouvea, C. P., Lidizio, L. R., et al. (2017). Al-/Fe-(hydr)oxides–organic carbon associations in Oxisols — From ecosystems to submicron scales. *Catena, 154,* 63–72. https://doi.org/10.1016/j.catena.2017.02.017

Sparrow, L. A., & Uren, N. C. (2014). Manganese oxidation and reduction in soils: Effects of temperature, water potential, pH and their interactions. *Soil Research, 52*(5), 483–494. https://doi.org/10.1071/SR13159

USEPA. (2007). *Method 6200: Field portable X-ray fluorescence spectrometry for the determination of elemental concentrations in soil and sediment*. https://www.epa.gov/sites/production/files/2015-12/documents/6200.pdf

Wallis, C. M., & Walker, M. T. (1999). Field XRF analysis of arsenic and lead in soils at a former smelter facility. *Journal American Society of Mining and Reclamation*, *1999*(1), 52–59. https://doi.org/10.21000/JASMR99010052

Weindorf, D. C., Bakr, N., & Zhu, Y. (2014). Advances in portable X-ray fluorescence (PXRF) for environmental, pedological, and agronomic applications. *Advances in Agronomy, 128*. Elsevier. https://doi.org/10.1016/B978-0-12-802139-2.00001-9

Weindorf, D. C., & Chakraborty, S. (2016). Portable X-ray fluorescence spectrometry analysis of soils. *Methods of Soil Analysis*, *1*(1). https://doi.org/10.2136/methods-soil.2015.0033

Wright, R. J., & Stuczynski, T. (1996). Atomic Absorption and Flame Emission Spectrometry. In D. L. Sparks, A. L. Page, P. A. Helmke, & R. H. Loeppert (Eds.), *Methods of Soil Analysis Part 3 – Chemical Methods* (pp. 65–90). Madison, WI: SSSA, ASA. https://doi.org/10.2136/sssabookser5.3.c4

Yeomans, J. C., & Bremner, J. M. (1988). A rapid and precise method for routine determination of organic carbon in soil1. *Communications in Soil Science and Plant Analysis, 19,* 1467–1476. https://doi.org/10.1080/00103628809368027

Zago, V. C. P., das Dores, N. C., & Watts, B. A. (2019). Strategy for phytomanagement in an area affected by iron ore dam rupture: A study case in Minas Gerais State, Brazil. *Environmental Pollution, 249,* 1029–1037. https://doi.org/10.1016/j.envpol.2019.03.060